

A note on the short crack behavior at elongated notch roots

Jaime Tupiassú Pinho de Castro, jtcastro@puc-rio.br
Marco Antonio Meggiolaro, meggi@puc-rio.br
Antonio Carlos de Oliveira Miranda, amiranda@tecgraf.puc-rio.br
Pontifical Catholic University of Rio de Janeiro, Brazil

Hao Wu, hao.wu@polytech-lille.net
Abdellatif Imad, abdellatif.imad@polytech-lille.fr
Benseddiq Nouredine, nouredine.benseddiq@univ-lille1.fr
Université des Sciences et Technologies de Lille, France

Abstract

The notch sensitivity factor q used to quantify the influence of notches on fatigue strength has been associated with tiny non-propagating cracks at their roots, but the q plots used in practice are based on semi-empirical simplistic estimates which do not recognize such cracks. By modeling the influence of the notch tip stress gradient on the fatigue propagation of mechanically short cracks, it is shown that those traditional q plots are only applicable to semicircular notches. Elongated semi-elliptical slits, on the other hand, can have very different q values which depend on the notch shape, not only on its tip radius. These predictions are supported by measuring the fatigue crack re-initiation lives after drilling a hole at the tip of deep pre-cracks on modified SE(T) specimens, to force them to behave like an elongated notch.

Keywords: notch sensitivity, short cracks, fatigue life prediction, non-propagating cracks, fatigue resistance of notched materials

1. Introduction

The notch sensitivity factor $0 \leq q \leq 1$ is widely used in structural design to quantify the difference between K_t , the linear elastic stress concentration factor (SCF) of a notch, and K_f , its corresponding fatigue SCF, used to quantify the actual notch effect on the fatigue strength [1]. In this way, if $K_t = \sigma_{max}/\sigma_n$, where σ_{max} is the maximum (linear elastic) stress at the notch root, and if σ_n is the nominal stress that would act at that point if the notch did not affect the stress field around the notch, the fatigue SCF is defined by

$$K_f = 1 + q \cdot (K_t - 1) = S'_L / S_{Lnt} \quad (1)$$

where S'_L and S_{Lnt} are the fatigue limits (or else the fatigue strengths at a given life) measured on smooth and on notched SN specimens, respectively.

It is well known that, at least in undamaged compact materials, q can be associated with the relatively fast generation of tiny non-propagating fatigue cracks at notch roots, see Fig. 1. Indeed, according to Frost [2], early evidence that small non-propagating fatigue cracks are found at notch roots when $2S'_L/K_t < \Delta\sigma_n < 2S'_L/K_f$ (at least in metallic alloys) goes back as far as 1949. Therefore, it is certainly reasonable to expect that such cracks can quantitatively explain why $K_f \leq K_t$ and, consequently, that the notch sensitivity can be analytically predictable from the fatigue propagation behavior of short cracks emanating from its tip. The purpose of this work is to demonstrate that in fact this can be done using relatively simple but sound mechanical principles, which do not require heuristic arguments.

To achieve this task, first the influence of the stress field gradient ahead the notch roots on the propagation of short fatigue cracks is studied, in order to associate the notch sensitivity to

the transition between their non-propagating and propagating states. Knowing that for stress analysis purposes notches of depth b and tip radius ρ can be supposed elliptical with semi-axis b and c and tip radius $\rho = c^2/b$, it is shown that for a given material q depends not only on ρ , but also very much on the ratio c/b [3-4]. It is also shown that the material influence on the notch sensitivity depends on its propagation threshold for (long) fatigue cracks ΔK_0 and on its fatigue limit for crack initiation ΔS_0 measured under pulsating loads at $R = \sigma_{min}/\sigma_{max} = 0$. Finally, the predicted q values are verified by fatigue testing several Al 6082 T6 notched specimens. It should be noted that “short crack” here means “mechanically short crack” not “microstructurally short crack”, since material isotropy is assumed in their modeling, a simplified hypothesis corroborated by the measured experimental results.

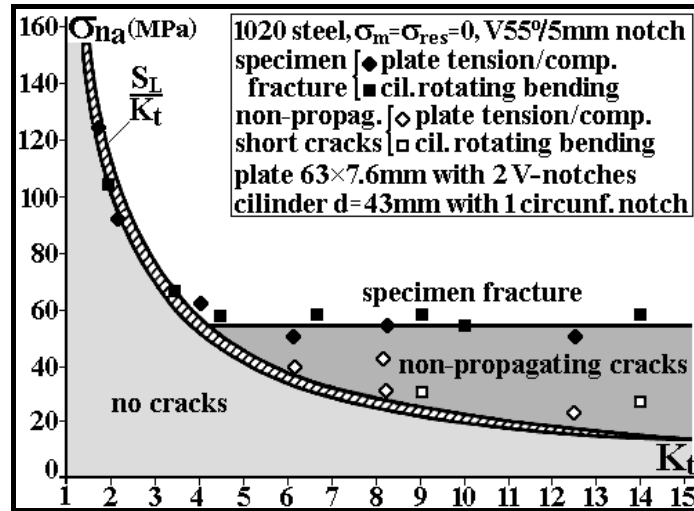


Fig. 1: Classical data showing that non-propagating fatigue cracks are generated at the notch roots if $2S'_L/K_t < \Delta\sigma_n < 2S'_L/K_f$ [2].

2. The propagation of (mechanically) short fatigue cracks

The fatigue crack propagation (FCP) threshold of short cracks must be smaller than ΔK_0 , otherwise the stress range $\Delta\sigma$ required to propagate them would be higher than ΔS_0 . Indeed, as the stress intensity factor (SIF) range $\Delta K \approx \Delta\sigma\sqrt{\pi a}$ controls the FCP process, if short cracks with $a \rightarrow 0$ had the same ΔK_0 threshold of the long cracks, then their propagation by fatigue would require $\Delta\sigma \rightarrow \infty$, a physical non-sense. For a good review of near-threshold FCP see e.g. Lawson et al [5].

The crack size influence on the propagation threshold $\Delta K_{th}(a)$ of short fatigue cracks can be modeled using El Haddad-Topper-Smith's (ETS) short crack characteristic value a_0 , estimated from ΔS_0 and ΔK_0 [6]. This clever trick reproduces well the Kitagawa-Takahashi [7] plot trend, see Fig. 2, using a modified SIF range $\Delta K'$ to describe the fatigue propagation of any crack, where

$$\Delta K' = \Delta\sigma\sqrt{\pi(a+a_0)}, \text{ where } a_0 = (1/\pi)(\Delta K_0/\Delta S_0)^2 \quad (2)$$

Using this a_0 trick, it is indeed possible to reproduce the expected limits $\Delta K_{th}(a \rightarrow \infty) = \Delta K_0$ and $\Delta\sigma(a \rightarrow 0) = \Delta S_0$, see Fig. 2. Knowing that steels typically have $6 < \Delta K_0 < 12 \text{ MPa}\sqrt{\text{m}}$, ultimate tensile strength $400 < S_U < 2000 \text{ MPa}$ and fatigue limit $200 < S'_L < 1000 \text{ MPa}$ (as very clean high-strength steels tend to maintain the usual $S'_L \cong S_U/2$ trend measured in lower strength steels under fully alternated loads, at an R-ratio $R = -1$) - and estimating by Good-

man $\Delta S_0 = 2S_U S'_L / (S_U + S'_L) \Rightarrow 260 < \Delta S_0 < 1300 \text{ MPa}$ - it can be expected that the maximum ETS a_0 range for steels is given by

$$(1/\pi)(\Delta K_{0min} / \Delta S_{0max})^2 \cong 7 < a_0 < 700 \mu\text{m} \cong (1/\pi)(\Delta K_{0max} / \Delta S_{0min})^2 \quad (3)$$

This a_0 range is probably overestimated, since the minimum threshold ΔK_{0min} is not necessarily associated with the maximum fatigue crack initiation limit ΔS_{0max} , nor ΔK_{0max} is associated with ΔS_{0min} . But it nevertheless justifies the “short crack” denomination used for cracks of a similar small size, and highlights the short crack dependence on the FCP threshold and on the fatigue limit of the material.

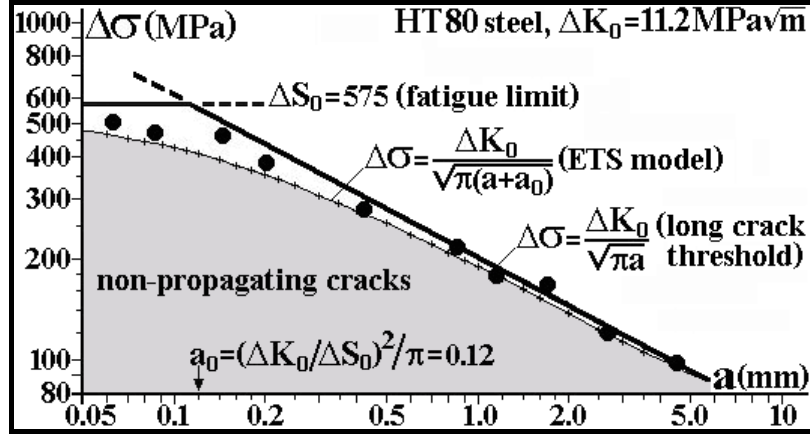


Fig. 2: Kitagawa-Takahashi plot describing the fatigue propagation of short and long cracks under $R = 0$ in a HT80 steel with $\Delta K_0 = 11.2 \text{ MPa}\sqrt{\text{m}}$ and $\Delta S_0 = 575 \text{ MPa}$ [6]: long cracks with $a \gg a_0$ stop when $\Delta\sigma \leq \Delta K_0 / \sqrt{\pi a}$, very short cracks with $a \ll a_0$ stop when $\Delta\sigma \leq \Delta S_0$, and the ETS curve predicts crack stop when $\Delta\sigma \leq \Delta K_0 / \sqrt{\pi(a + a_0)}$.

As the typical strengths of aluminum alloys are $70 < S_U < 600 \text{ MPa}$, $30 < S'_L < 230 \text{ MPa}$, $40 < \Delta S_0 < 330 \text{ MPa}$ and $1.2 < \Delta K_0 < 5 \text{ MPa}\sqrt{\text{m}}$, their maximum a_0 (over)estimated range, and thus their short crack influence scale, is wider than the steels range, $1 \mu\text{m} < a_0 < 5 \text{ mm}$.

Since equation (2) is deduced using the SIF $\Delta K = \Delta\sigma\sqrt{\pi a}$ of the Irwin's plate, Yu *et al* [8] and Atzori *et al* [9] used the geometry factor α of the general expression $\Delta K = \Delta\sigma\sqrt{\pi a} \cdot \alpha$ to deal with other geometries, defining

$$\Delta K'_I = \alpha \cdot \Delta\sigma \sqrt{\pi(a + a_0)}, \quad \text{where } a_0 = (1/\pi) \left[\Delta K_0 / (\alpha \cdot \Delta S_0) \right]^2 \quad (4)$$

This expression implies that $\Delta\sigma$ tends to the fatigue limit ΔS_0 if $a \rightarrow 0$, which is only true when $\Delta\sigma$ is the notch root stress range, instead of the nominal stress. However, in most cases the geometry factor α found in SIF tables already includes the effects of the notch root SCF, defining $\Delta\sigma \equiv \Delta\sigma_n$ as the nominal stress. Hence, a clearer way to define the short crack length parameter a_0 when the crack departs from a notch is to follow this practice considering as usual $\Delta\sigma$ to be the nominal stress range and separating the geometry factor α into two parts: $\varphi(a)$, which tends to the notch root SCF as the crack length a tends to zero, and η , which only encompasses the remaining terms, such as the free surface correction:

$$\Delta K' = \eta \cdot \varphi(a) \cdot \Delta\sigma \sqrt{\pi(a + a_0)}, \quad \text{where } a_0 = (1/\pi) \left[\Delta K_0 / (\eta \cdot \Delta S_0) \right]^2 \quad (5)$$

Note that the first factor $\varphi(a)$ does not appear in this expression for a_0 , because for very small cracks ($a \rightarrow 0$) the notch root stress range $\varphi(0) \cdot \Delta\sigma$ should be equal to ΔS_0 .

Alternatively, the short crack problem can be probably more clearly modeled by letting the SIF range ΔK retain its original equation, while the threshold expression is modified to become a function of the crack length a , namely $\Delta K_{th}(a)$, resulting in

$$\Delta K_{th}(a)/\Delta K_0 = \sqrt{a/(a+a_0)} \quad (6)$$

The El Haddad-Topper-Smith's equation can be seen as one possible asymptotic match between the short and long crack behaviors. Following Bazant's [10] reasoning, a more general equation can be used introducing an adjustable parameter γ to fit experimental data

$$\Delta K_{th}(a)/\Delta K_0 = \left[1 + (a_0/a)^{\gamma/2}\right]^{-1/\gamma} \quad (7)$$

Equations (2-6) are obtained from (7) when $\gamma = 2.0$, and the bi-linear limit estimate given by $\Delta\sigma(a \leq a_0) = \Delta S_0$ for short cracks and $\Delta K_{th}(a \geq a_0) = \Delta K_0$ for long ones shown in Fig. 2 is obtained if $\eta \cdot \varphi(a) = 1$ and $\gamma \rightarrow \infty$. The fitting parameter γ allows this $\Delta K_{th}(a)$ estimate to better fit short crack propagation data from Tanaka et al [11] and Livieri and Tovo [12], see Fig. 3. Most data in this figure is bounded by the curves obtained using $\gamma = 1.5$ and $\gamma = 8$.

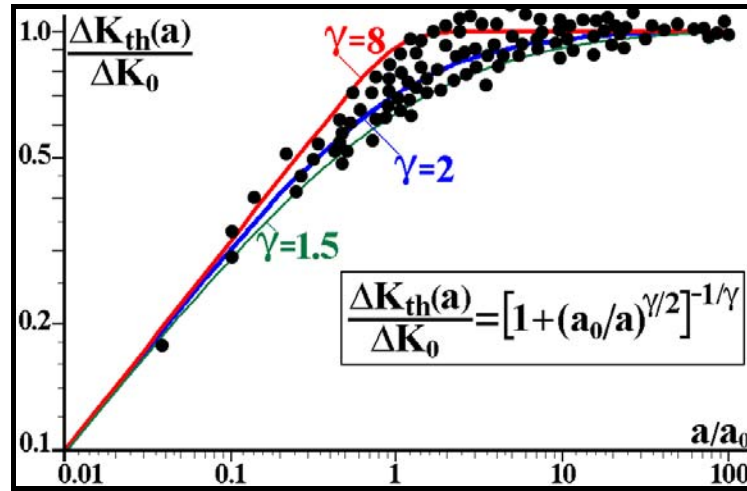


Fig. 3: Ratio between short and long crack propagation thresholds as a function of a/a_0 .

In the following sections, these ideas are first applied to predict the propagation behavior of short cracks emanating from circular holes, and then extended to describe the behavior of cracks which depart from semi-elliptical notches, resulting in improved estimates of the notch sensitivity q and of the largest non-propagating crack size tolerated at such notch tips.

3. The behavior of short cracks which depart from circular holes

The FCP behavior of short cracks emanating from circular holes in Kirsch (infinite) plates is now evaluated. The SIF of a single crack with length a emanating from a circular hole with radius ρ in an infinite plate loaded by a tensile stress range $\Delta\sigma$ is expressed, within 1%, by

$$\Delta K = 1.12 \cdot \varphi(a/\rho) \cdot \Delta\sigma \sqrt{\pi a} \quad (8)$$

where the factor $\varphi(a/\rho) \equiv \varphi(x)$, related to the hole stress concentration, is given by [13]

$$\varphi(x) = \left(1 + \frac{0.2}{(1+x)} + \frac{0.3}{(1+x)^6}\right) \cdot \left(2 - 2.354 \frac{x}{1+x} + 1.2056 \left(\frac{x}{1+x}\right)^2 - 0.2211 \left(\frac{x}{1+x}\right)^3\right), \quad x \equiv \frac{a}{\rho} \quad (9)$$

Note that when the crack size a tends to zero, equation (8) becomes

$$\lim_{a \rightarrow 0} \Delta K = 1.12 \cdot 3 \cdot \Delta \sigma \sqrt{\pi a} \quad (10)$$

as expected, since it combines the solution for an edge crack in a semi-infinite plate with the SCF of a circular Kirsch hole, which has $K_t = \varphi(0) = 3$. Note also that the other limit, for the long cracks with $a \gg a_0$, results in

$$\lim_{a \rightarrow \infty} \Delta K = \Delta \sigma \sqrt{\pi a / 2} \quad (11)$$

which is the SIF for a long crack with length a in an infinite plate, where the crack tip is so far from the hole that it does not suffer its influence in the stress field (note the equivalent crack length is $a + 2\rho$, however as $a \rightarrow \infty$ the ρ value disappears from the equation). Thus, the SIF of a long crack which departs from a Kirsch hole has $\varphi(x \rightarrow \infty) = 1/1.12 \sqrt{2} \cong 0.63$.

Using equation (7) to express the FCP threshold, it can then be stated that any crack departing from a Kirsch hole will propagate when

$$\Delta K = \eta \cdot \varphi(a/\rho) \cdot \Delta \sigma \sqrt{\pi a} > \Delta K_{th}(a) = \Delta K_0 \cdot \left[1 + (a_0/a)^{\gamma/2} \right]^{-1/\gamma} \quad (12)$$

where $\eta = 1.12$ is the free surface correction. Knowing that $\Delta K_{th} \equiv \Delta K_0$ for a long crack, the crack length parameter a_0 from the above equation is

$$a_0 = (1/\pi) \left[\Delta K_0 / (1.12 \cdot \Delta S_0) \right]^2 \quad (13)$$

Note that, as discussed before, the factor $\varphi(a/\rho)$ does not appear in the definition of a_0 . Therefore, the crack propagation criterion can be based on dimensionless functions $\varphi(a/\rho)$ and $g(a/\rho, \Delta S_0/\Delta \sigma, \Delta K_0/\Delta S_0 \sqrt{\rho}, \gamma)$ [14], and re-written as

$$\varphi\left(\frac{a}{\rho}\right) > \frac{(\Delta K_0 / \Delta S_0 \sqrt{\rho}) \cdot (\Delta S_0 / \Delta \sigma)}{\left[(\eta \sqrt{\pi a / \rho})^\gamma + (\Delta K_0 / \Delta S_0 \sqrt{\rho})^\gamma \right]^{1/\gamma}} \equiv g\left(\frac{a}{\rho}, \frac{\Delta S_0}{\Delta \sigma}, \frac{\Delta K_0}{\Delta S_0 \sqrt{\rho}}, \gamma\right) \quad (14)$$

In other words, if $x \equiv a/\rho$ and $\kappa \equiv \Delta K_0/\Delta S_0 \sqrt{\rho}$, a fatigue crack departing from a Kirsch hole grows whenever $\varphi(x) > g(x, \Delta S_0/\Delta \sigma, \kappa, \gamma) \Rightarrow \varphi/g > 1$. Fig. 4 plots some φ/g functions for several fatigue strength to loading stress range ratios $\Delta S_0/\Delta \sigma$ as a function of the normalized crack length $x \equiv a/\rho$, assuming a material/notch combination with $\kappa = 1.5$ and $\gamma = 6$ [15].

For high applied stress ranges $\Delta \sigma$, the strength to load $\Delta S_0/\Delta \sigma$ ratio is small, and the corresponding φ/g curve is always higher than 1, meaning that cracks will initiate and propagate from the Kirsch hole border, without stopping during this process. One example of such a case is the upper curve in Fig. 4, which shows the function $\varphi/g_{1.4}$ obtained for $\Delta S_0/\Delta \sigma = 1.4$. On the other hand, small stress ranges $\Delta \sigma$ with load ratios $\Delta S_0/\Delta \sigma \geq K_t = 3$ have φ/g functions which are smaller than 1, meaning that no crack will initiate from the Kirsch hole, and that small enough cracks will not propagate from it at such low loads. This is illustrated by curves φ/g_3 , associated with the limit case $\Delta S_0/\Delta \sigma = 3$, and φ/g_4 , associated with $\Delta S_0/\Delta \sigma = 4$.

But three other cases must be noted in Fig. 4. The first crosses once the $\varphi/g = 1$ line, see the $\varphi/g_{2.3}$ curve, meaning such an intermediate load range can initiate and propagate a fatigue crack from the notch border until the decreasing $\varphi/g_{2.3}$ value reaches 1, where the crack stops. Thus, this loading level generates a non-propagating fatigue crack at the notch border due to the crack tip stress gradient effect, with a size given by the corresponding $a = x \cdot \rho$ abscissa.

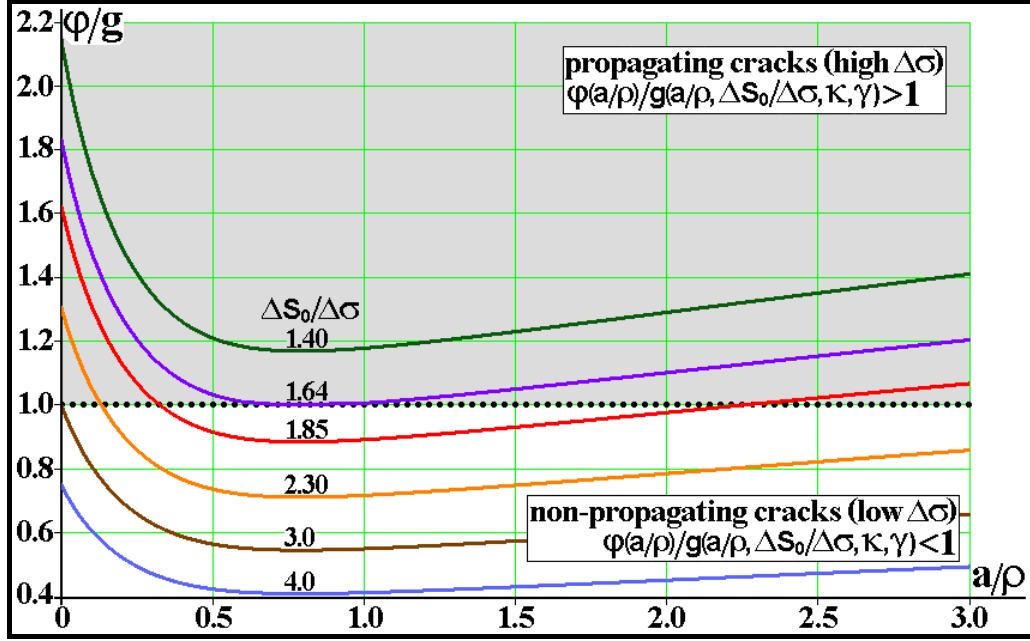


Fig. 4: The fatigue stress concentration factor K_f can be obtained by finding the function φ/g which is tangent to the $\varphi/g = 1$ line, thus in this case $K_f = 1.64$.

The second, illustrated in Fig. 4 by the $\varphi/g_{1.85}$ curve, intersects the $\varphi/g = 1$ line twice. Therefore, this load level will also generate a fatigue crack at the Kirsch hole border, which will propagate until reaching the maximum size obtained from the abscissa of the first intersection point (on the left), where the crack stops. Moreover, cracks longer than the size defined by the abscissa of the second intersection point will re-start propagating by fatigue under $\Delta\sigma = \Delta S_0/1.85$ until eventually fracturing the Kirsch plate. However, the crack initiated by fatigue under such load cannot propagate between these two intersection points by fatigue alone (assuming $\Delta\sigma$ remains constant). Hence, it can only grow in this region if driven by a different mechanism, such as corrosion or creep, for example.

These two cases seem different, yet they are similar: the $\varphi/g_{2.3}$ curve will cross the $\varphi/g = 1$ line twice if the graph is extended to larger $x \equiv a/\rho$ values, because a sufficiently long crack can always propagate by fatigue under a given (even if small) $\Delta\sigma$ range whenever its SIF range $\Delta K = \alpha \cdot \Delta\sigma \sqrt{\pi a}$ grows with the crack size a , as in this Kirsch plate. In fact, all φ/g curves start at $K_t \Delta\sigma / \Delta S_0$ and $a = 0$, and become higher than 1 for sufficiently large a/ρ values.

Finally, the $\varphi/g_{1.64}$ curve is tangent to the $\varphi/g = 1$ line, meaning that this $\Delta\sigma = \Delta S_0/1.64$ is the smallest stress range that can cause crack initiation and propagation without arrest from the notch border. In other words, by definition, the Fig. 4 Kirsch hole fatigue SCF is given by $K_f = \Delta S_0 / \Delta\sigma = 1.64$. Moreover, the abscissa x_{max} of the tangency point between the $\varphi/g_{1.64}$ curve and the $\varphi/g = 1$ line gives the largest non-propagating crack that can arise from it by fatigue alone, $a_{max} = x_{max} \cdot \rho$. Therefore, the K_f and a_{max} can be found by solving the system

$$\begin{cases} \varphi/g = 1 \\ \partial(\varphi/g)/\partial x = 0 \end{cases} \Rightarrow \begin{cases} \varphi(x_{max}) = g(x_{max}, K_f, \kappa, \gamma) \\ \partial\varphi(x_{max})/\partial x = \partial g(x_{max}, K_f, \kappa, \gamma)/\partial x \end{cases} \quad (15)$$

This system can be solved numerically for each combination of $\kappa \equiv \Delta K_0 / \Delta S_0 \sqrt{\rho}$ and γ values, and the notch sensitivity factor q is then obtained from

$$q(\kappa, \gamma) \equiv (K_f(\kappa, \gamma) - 1) / (K_t - 1) \quad (16)$$

Thus, the notch sensitivity q can be calculated using appropriate analytical procedures, without appealing to semi-empirical heuristic arguments, by quantifying how the stress gradient at the notch root affects the short crack propagation, including the material-dependent data fit parameter γ influence on $\Delta K_{th}(a)$. Moreover, this approach can be easily extended to semi-elliptical notches, which can be analyzed in the same way, as shown in the following section.

4. The physical behavior of short cracks which depart from elongated notches

Before jumping into more elaborated mechanical procedures, it is worth to present a simple and unambiguous explanation for why a crack can start from a sharp notch root and propagate for a while before stopping and becoming non-propagating (under fixed loading conditions), in order to enhance the advantages of the model proposed here.

A very reasonable estimate for the SIF of a small crack $a \ll b$ which departs from the tip of an elliptical notch with semi-axes b and c and root radius $\rho = c^2/b$ in an Inglis plate, with the $2b$ axis centered at the x coordinate origin, is $K_I(a) \cong \sigma_n \cdot \sqrt{(\pi a)} f_1(a, b, c) f_2(\text{free surface})$, where σ_n is the nominal stress (perpendicular to a and b); $f_1(a, b, c) \cong \sigma_y(x)/\sigma_n$; $\sigma_y(x)$ is the stress that acts at the point $(x = b + a, y = 0)$ in front of the notch root when there is no crack; and $f_2 = 1.12$. The more slender the elliptical notch, meaning the smaller their c/b ratio and tip radius ρ , the higher are its K_t and the stress gradient near its tip, thus the faster the $\sigma_y(x)/\sigma_n$ ratio drops. The distribution of the $\sigma_y(x)$ is given by [16]:

$$f_1 = \frac{\sigma_y(x=b+a, y=0)}{\sigma_n} = 1 + \frac{(b^2 - 2bc)(x - \sqrt{x^2 - b^2 + c^2})(x^2 - b^2 + c^2) + bc^2(b-c)x}{(b-c)^2(x^2 - b^2 + c^2)\sqrt{x^2 - b^2 + c^2}} \quad (17)$$

The peculiar growth of short cracks which depart from elliptical notch roots is caused by the usually sharp stress gradient there: the linear elastic stress concentration induced by any elliptical hole with $b \geq c$ drops from $K_t = 1 + 2b/c = 1 + 2\sqrt{b/\rho} = \sigma_y(1)/\sigma_n \geq 3$ at its tip surface to a value $1.82 < K_{1.2} = \sigma_y(1.2)/\sigma_n < 2.11$ at a point just $b/5$ ahead of it, see Fig. 5. Thus, when the notch is slender and has a high K_t , the SIF of those short cracks, which in principle should tend to increase with their length $a = x - b$, may instead decrease after they grow for a while, since the K_t affected stress in $K_I \cong 1.12 \cdot \sigma_n \sqrt{(\pi a)} f_1$ may decrease sharply due the high stress gradient there, overcompensating the crack growth effect, see Fig. 6.

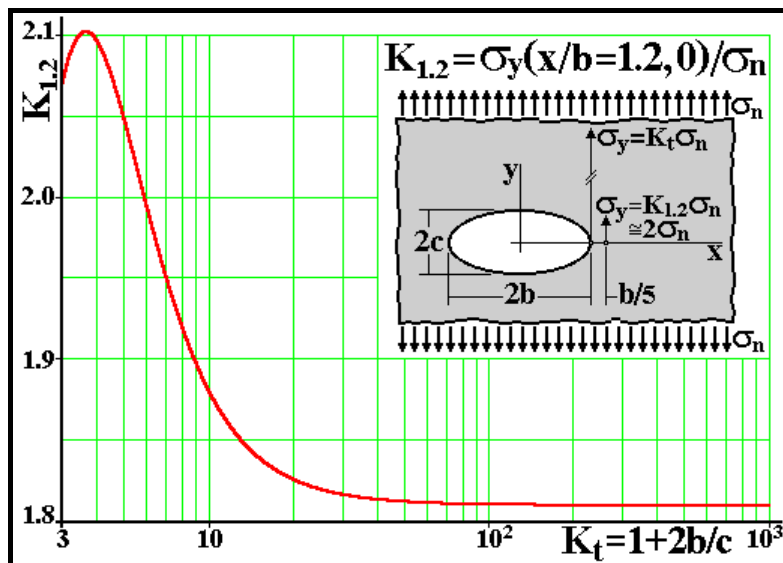


Fig. 5: The ratio $K_{1.2} = \sigma_y(x/b = 1.2, 0)/\sigma_n$ at just $b/5$ ahead of the tip of elliptical Inglis holes is almost independent of its linear elastic SCF $K_t = 1 + 2b/c = 1 + 2\sqrt{b/\rho}$.

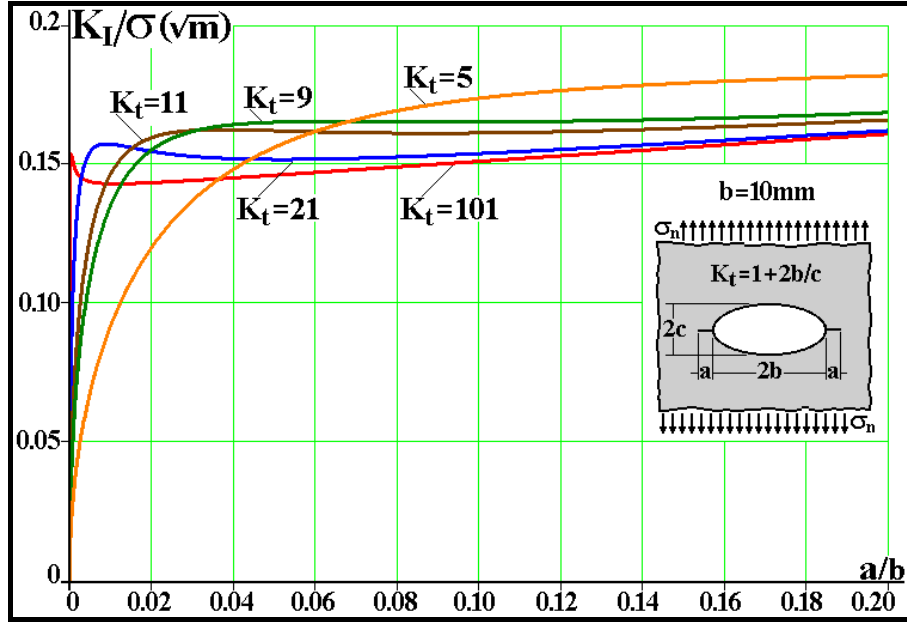


Fig. 6: The estimate $K_I \cong 1.12 \cdot \sigma_n \sqrt{\pi a} f_I(K_t, a)$ for the cracks which depart from the tips of an Inglis elliptical hole with $b = 10\text{mm}$ illustrate how the derivative $\partial K_I / \partial a$ may decrease sharply just after the cracks initiate there.

This $K_I(a)$ estimate can be used to evaluate the non-propagating fatigue cracks tolerable at notch roots, using the short crack propagation behavior. A simple numerical example clarifies this point: if a large steel plate with $S_U = 600\text{MPa}$, $S_L = 200\text{MPa}$ and $\Delta K_0 = 9\text{MPa}\sqrt{\text{m}}$ works under an alternated load range $\Delta\sigma_n = 100\text{MPa}$ at $R = -1$, $K_I(a)$ let verify if it is possible to change an originally circular $d = 20\text{mm}$ central hole by an elliptical one with $2b = 20\text{mm}$ (perpendicular to σ_n) and $2c = 2\text{mm}$, without inducing the plate to fail by fatigue.

Neglecting the buckling problem, which can be important in a thin plate, the circular hole is safe, since it has a fatigue crack initiation safety factor $\phi_F = S_L / K_f \cdot \sigma_n = 200 / 150 \cong 1.33$, as this large hole has $K_f \cong K_t = 3$, $\sigma_n = \Delta\sigma_n / 2$, and S_L includes the necessary modification factors to consider surface roughness and similar effects on the plate fatigue limit. But by traditional SN procedures the elliptical hole would not be admissible, as it has a high $K_t = 1 + 2b/c = 21$ and a small tip radius $\rho = c^2/b = 0.1\text{mm}$, thus a notch sensitivity estimated from the usual Peterson q plot [1] $q \cong 0.32$, which would induce $K_f = 1 + q(K_t - 1) = 7.33$, and therefore a maximum load amplitude $K_f \cdot \sigma_n = 376\text{MPa} > S_L$. However, as this K_f value is considerably higher than typical values reported in the literature [15-18], it is worth to re-study this simple problem considering the short crack propagation behavior.

Supposing $\Delta K_{th}(R < 0) \cong \Delta K_0$, assuming as usual that a fatigue crack does not propagate while closed, and estimating $\Delta K_{th}(a) = \Delta K_0 / [1 + (a_0/a)]^{-0.5}$ (by ETS), $S'_L = 0.5S_R$ (the material fatigue limit, as FCP modeling does not require the modifying factors necessary to estimate S_L), $\Delta S_0 = S_R / 1.5$ (by Goodman) and $a_0 = (1/\pi)(1.5\Delta K_0 / 1.12 \cdot S_R)^2 \cong 0.13\text{mm}$, the SIF ranges $\Delta K_I(a)$ for the two holes are compared to the propagation threshold $\Delta K_{th}(a)$, see Fig. 7.

This figure shows that the SIF range $\Delta K_I(a)$ curve for cracks departing from the 20mm diameter circular notch remains below the $\Delta K_{th}(a)$ FCP threshold curve which considers the short crack behavior up to $a \cong 1.54\text{mm}$. Thus, if a small superficial scratch locally augments the maximum stresses at that hole border under $\Delta\sigma_n = 100\text{MPa}$ and $R = -1$ up to the point it initiates a tiny crack, this crack would have no tendency to propagate under this (fixed) load, confirming its “safe” prediction made above by traditional SN fatigue design procedures.

However, if a crack with $a > 1.54\text{mm}$ is introduced at this Kirsch hole border by any other means, it would then propagate by fatigue under those otherwise safe loading conditions, as $\Delta K_I(a)$ values are greater than the material FCP resistance $\Delta K_{th}(a)$ after this intersection point.

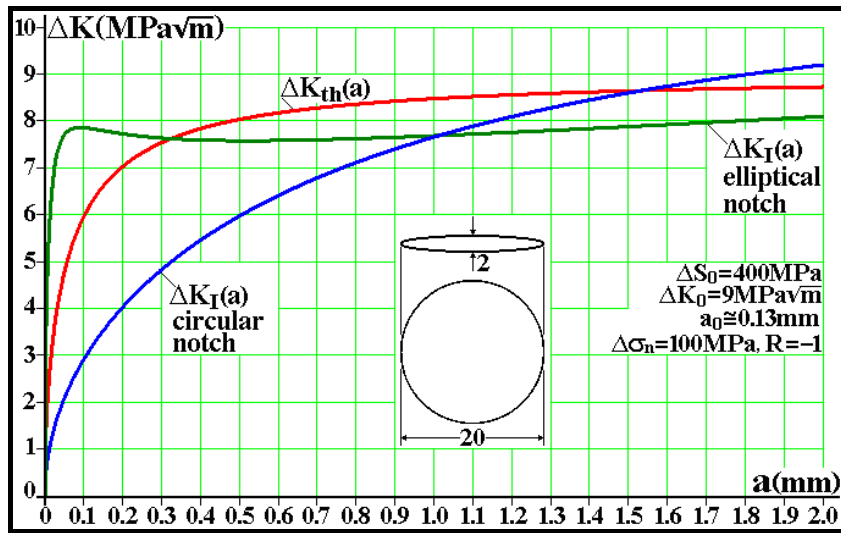


Fig. 7: Cracks do not initiate at the circular hole, which tolerates cracks $a < 1.54\text{mm}$, while the crack which initiates at the elliptical notch tip stops after reaching $a \cong 0.33\text{mm}$.

On the other hand, under these same $\Delta\sigma_n = 100\text{MPa}$ and $R = -1$ loading conditions, the $\Delta K_I(a)$ curve for the elliptical hole starts above $\Delta K_{th}(a)$, meaning that a crack should initiate at its tip, as expected from its high K_t . However, as this tiny crack propagates through the high stress gradient ahead of the notch root, it sees fast diminishing stresses at its tip during its early growth. This decreasing stress field overcompensate the increasing crack size effect on $\Delta K_I(a)$ until it eventually becomes smaller than $\Delta K_{th}(a)$ at $a \cong 0.33\text{mm}$, when the crack stops, becoming non-propagating (if the nominal $\Delta\sigma_n$ and R loading remains fixed), see Fig. 7.

Since a terminal fatigue failure includes crack initiation and growth up to fracture, in this sense both the circular and the elliptical notches could be considered safe for the assumed plate service loading. However, the non-propagating crack at the elliptical notch tip, a clear evidence of fatigue damage, renders it much less robust than the circular one. For example, a small 10% increment in $\Delta\sigma_n$ could make the crack initiate and propagate from the elliptical notch until the plate fractures, while the circular notch would remain safe, still tolerating a crack $a \cong 1\text{mm}$, as shown in Fig. 8.

These conclusions are quite interesting, but they are based on estimates and thus cannot of course be used for design purposes. Nevertheless, as these estimation procedures are reasonably based on clear and sound mechanical hypothesis, which do not require heuristic arguments such as ill defined material dependent characteristic distances, they do justify the development of the more precise calculations presented in the following section.

5. The analysis of short cracks which depart from elongated notches

The logical reasoning used to model the notch sensitivity of the circular Kirsch hole can now be extended to model elliptical notches, which in turn can be used to model most elongated notches which have the same depth and tip radius. The SIF range of a single crack with length a emanating from a semi-elliptical notch with semi-axes b and c (where b is in the same direction as a) at the edge of a very large plate can be written as

$$\Delta K_I = \eta \cdot F(a/b, c/b) \cdot \Delta\sigma \sqrt{\pi a} \quad (18)$$

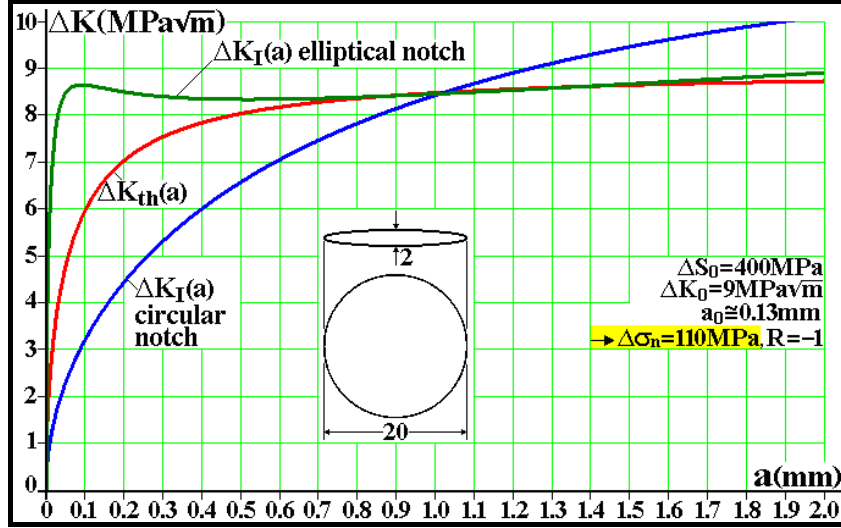


Fig. 8: The circular hole is much more robust than the elliptical notch: if the load is increased by just 10%, the crack initiated at the elliptical notch tip does not stop anymore, while the circular hole still tolerates a crack of size $a < \sim 1\text{mm}$ departing from its border.

where $\eta = 1.12$ is the free surface correction, and $F(a/b, c/b)$ is a geometry factor associated with the notch stress concentration, which can be expressed as a function of the dimensionless parameter $s = a/(b + a)$ and of the notch SCF

$$K_t = \left[1 + 2 \frac{b}{c} \right] \cdot \left[1 + \frac{0.12}{(1 + c/b)^{2.5}} \right] \quad (19)$$

To obtain expressions for F , Finite Element (FE) calculations were performed using the Quebra2D program [19] considering several cracked semi-elliptical notch configurations. The numerical results, which agreed well with standard solutions [13], were fitted within 3% using empirical equations, resulting in

$$F(a/b, c/b) \equiv f(K_t, s) = K_t \cdot \sqrt{\frac{1 - \exp(-K_t^2 \cdot s)}{K_t^2 \cdot s}}, \quad c \leq b \quad (20)$$

$$F(a/b, c/b) \equiv f'(K_t, s) = K_t \cdot [1 - \exp(-K_t^2)]^{-s/2} \cdot \sqrt{\frac{1 - \exp(-K_t^2 \cdot s)}{K_t^2 \cdot s}}, \quad c \geq b \quad (21)$$

where $s = a/(a + b)$. Fig. 9 shows how well equation (20) fits the $F(a/b, c/b)$ generated by the FE calculations. Similar results are found for equation (21) [14].

Traditional notch sensitivity estimates assume that q depends only on the notch root ρ and on the material ultimate strength S_U . Thus, similar materials with the same S_U but different ΔK_0 should have identical notch sensitivities, according to these estimates. The same should occur with shallow and deep or elongated notches of identical tip radii. However, it must be mentioned that well established empirical relations relate the fatigue limit ΔS_0 to S_U , but there is no such relation between the FCP threshold ΔK_0 and S_U . Moreover, it is also important to point out that the q estimation for elongated notches by the traditional procedures can generate questionable K_f values, as discussed above.

The proposed model, on the other hand, recognizes that q values of semi-elliptical notches, besides depending on ρ , ΔS_0 , ΔK_0 and γ , are also strongly dependent on the c/b ratio, see Fig.

10. The curves shown in this figure are calculated for typical aluminum alloys which have mean $S_U = 225\text{MPa}$, fatigue limit $S_L = 90\text{MPa} \Rightarrow \Delta S_0 = 2S_L S_R / (S_L + S_R) = 129\text{MPa}$, propagation threshold $\Delta K_0 = 2.9\text{MPa}\sqrt{\text{m}}$, $\gamma = 6$, and short crack length parameter $a_0 = 0.26\text{mm}$. Their corresponding Peterson's curve is well approximated by the semi-circular $c/b = 1$ notch, but this curve is *not* applicable for high c/b ratios. Therefore, the proposed predictions indicate that these old estimates should not be used for elongated notches, a prediction experimentally verifiable, as discussed in the following section.

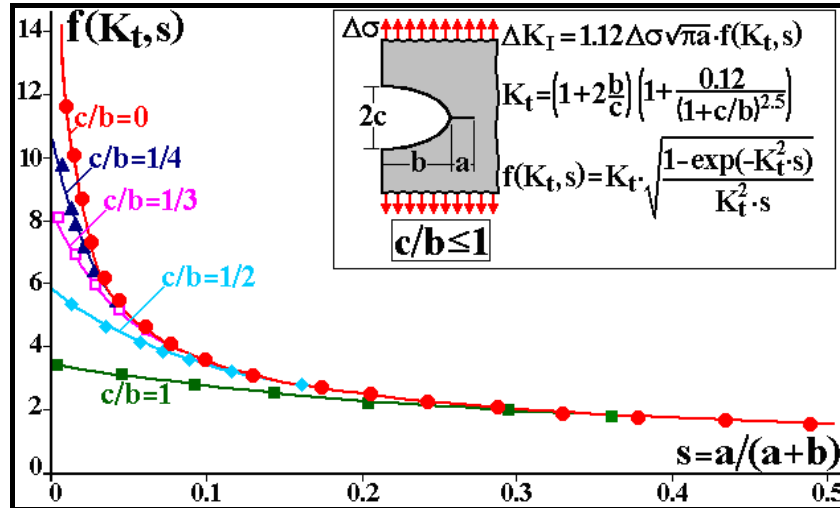


Fig. 9: Finite Element calculations and proposed fit for the geometry factor of semi-elliptical notches with $c \leq b$.

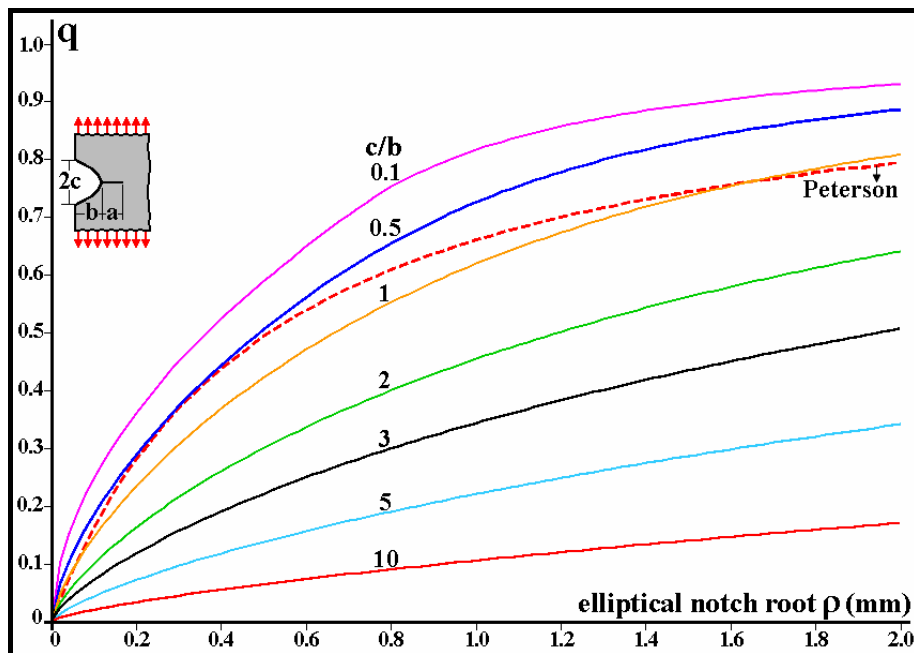


Fig. 10: Notch sensitivity q as a function of the semi-elliptical notch root radius $\rho = c^2/b$ for aluminum alloys having $a_0 = 0.26\text{mm}$ ($S_u \cong 225\text{MPa}$).

6. Experimental verification of the elongated notch sensitivity predictions

Fatigue tests were carried out on modified SE(T) specimens of thickness $B = 8\text{mm}$ and width $W = 80\text{mm}$ to find the number of cycles required to re-initiate the crack after drilling a stop-hole of radius ρ centred at its tip, generating an elongated slit with $b = 27.5\text{mm}$, as de-

tailed in [3,4]. Such tests can confirm the q model proposed here. The tested material was an Al alloy 6082 T6, with yielding strength $S_Y = 280\text{MPa}$, $S_U = 327\text{MPa}$ and Young's modulus $E = 68\text{GPa}$. The fatigue tests were performed at 30Hz under constant load range at $R = 0.57$, to avoid any crack closure influence on the FCP behavior. The fatigue crack re-initiation lives at the tip of the resulting elongated notch can be modeled by εN procedures using (i) Coffin-Manson's parameters $\sigma'_f = 485\text{MPa}$, $b = -0.0695$, $\varepsilon'_f = 0.733$ and $c = -0.827$, and Ramberg-Osgood's coefficient and exponent of the cyclic stress-strain curve, $K' = 443\text{MPa}$, $n' = 0.064$; (ii) the nominal stress range and R-ratio; and finally (iii) the stress concentration factor K_t of the notches generated after repairing the cracks by a stop-hole at their tips, which can be estimated by Inglis, giving for a stop-hole radius $\rho = 1 \Rightarrow K_t \cong 1 + 2\sqrt{a/\rho} = 11.49$.

The elongated slit can be modeled by first calculating the stress and strain maxima and ranges at its root by Neuber's stress/strain concentration rule, and by using them to calculate the crack re-initiation lives by an appropriate $\Delta\varepsilon \times N$ rule, considering the influence of the mean load. Neglecting this effect could lead to severely non-conservative predictions, as the R -ratio used in the tests was high (and indeed the Coffin-Manson predictions are highly non-conservative, thus absolutely useless in this case). Fig. 11 shows that the lives predicted by the elastic and by the elastic-plastic versions of Morrow's equation (Morrow El and Morrow EP) and by Smith-Topper-Watson (SWT) equation are similar in this case, but too conservative in comparison to the measured data. However, it is worth to emphasize that such a similarity cannot be assumed beforehand, since in many other cases these rules can predict very different fatigue lives!

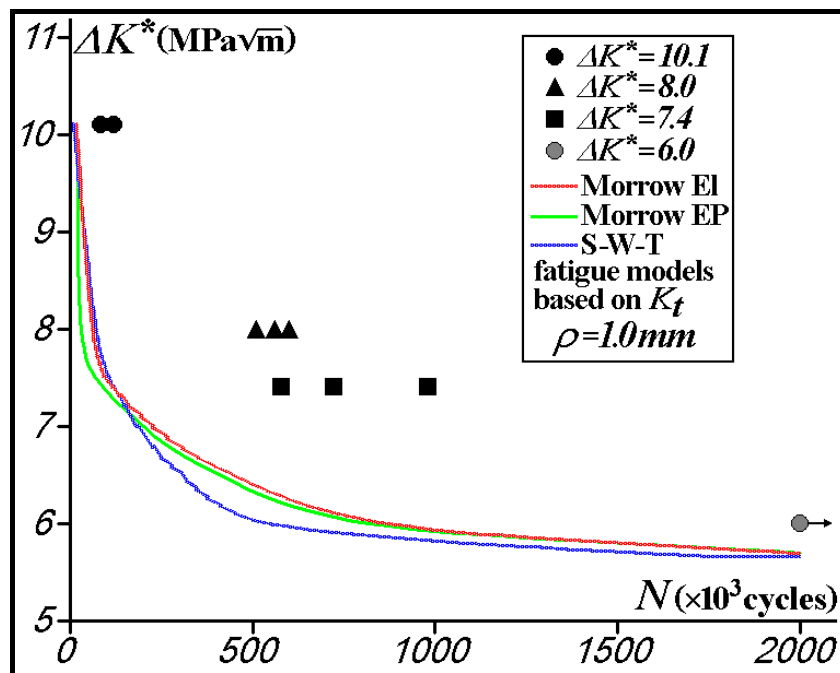


Fig. 11: Predicted and measured crack re-initiation lives after introducing the stop-holes with radii $\rho = 1.0\text{mm}$ at the tip of the crack in a SE(T) specimen, using the K_t of the resulting $b = 27.5\text{mm}$ elongated slit, modeled by the semi-elliptical notch which has the same length and tip radius.

However, when using K_f instead of K_t on the εN rules, calculating the elongated notch sensitivity q by the procedures discussed above, the predictions reproduce quite well the measured results, see Figure 12. The Al 6082 T6 fatigue limit and fatigue crack propagation threshold under pulsating loads required to calculate K_f are estimated as $\Delta K_0 = 4.8\text{MPa}\sqrt{\text{m}}$

and as $\Delta S_0 = 110\text{MPa}$, following traditional structural design practices. The Bazant's exponent was chosen as $\gamma = 6$, as recommended by [14].

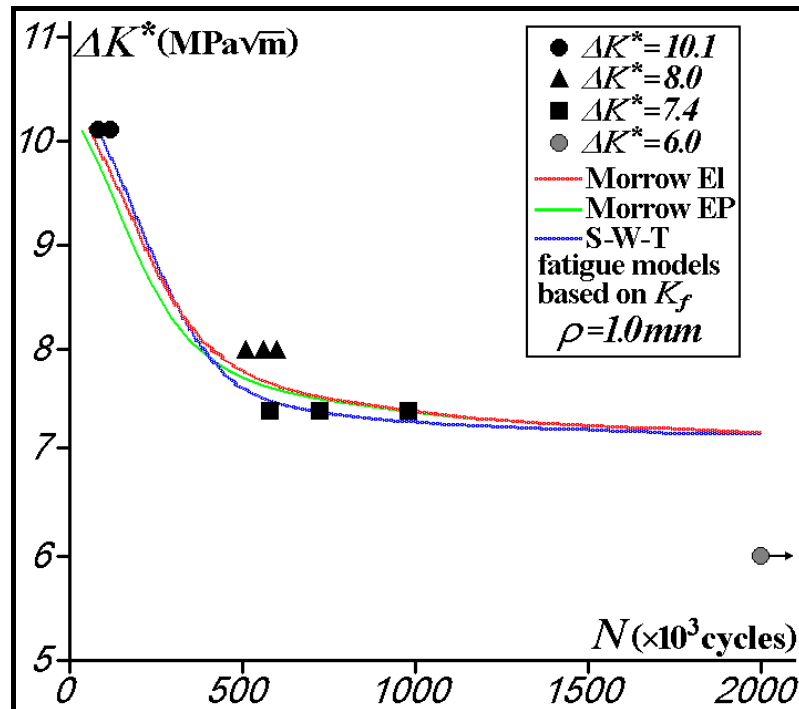


Fig. 12: Predicted and measured crack re-initiation lives after introducing the stop-holes with radii $\rho = 1.0\text{mm}$ at the tip of the crack in a SE(T) specimen, using the K_f of the resulting $b = 27.5\text{mm}$ elongated slit, estimated using the procedures proposed in this paper.

7. Conclusions

A generalized El Haddad-Topper-Smith's parameter was used to model the crack size dependence of the threshold stress intensity range for short cracks, as well as the behavior of non-propagating fatigue cracks. This dependence has been used to estimate the notch sensitivity factor q of semi-elliptical notches, from studying the propagation behavior of short non-propagating cracks that may initiate from their tips. The predicted notch sensitivities reproduce well the classical Peterson's q estimates for circular holes or approximately semi-circular notches, but it is found that the notch sensitivity of elongated slits has a very strong dependence on the notch aspect ratio, defined by the ratio c/b of the semi-elliptical notch that approximates the slit shape having the same tip radius. These predictions are confirmed by experimental measurements of the re-initiation life of long fatigue cracks repaired by introducing a stop-hole at their tips, using their calculated K_f and appropriate εN procedures.

8. Acknowledgements

CNPq has provided research scholarships for the Brazilian authors.

9. References

- [1] Peterson RE (1974) Stress Concentration Factors, Wiley.
- [2] Frost NE, Marsh KJ, Pook LP (1999) Metal Fatigue, Dover.
- [3] Wu H, Castro JTP, Imad A, Meggiolaro MA, Nourredine B (2009) in Mattos & Alves ed. Solid Mechanics in Brazil 2009, ABCM, ISBN 978-85-85769-43-7.

- [4] Wu H, Imad A, Nourredine B, Castro JTP, Meggiolaro MA (2009) On the prediction of the residual fatigue life of cracked structures repaired by the stop-hole method, *Int J Fatigue*, in press.
- [5] Lawson L, Chen EY, Meshii M (1999) Near-threshold fatigue: a review, *Int J Fatigue* 21:15-34.
- [6] El Haddad MH, Topper TH, Smith KN (1979) Prediction of non-propagating cracks, *Eng Fract Mech* 11:573-584.
- [7] Kitagawa H, Takahashi S (1976) Applicability of fracture mechanics to very small crack or cracks in the early stage, in *Proceedings of 2nd International Conference on Mechanical Behavior of Materials*, ASM.
- [8] Yu MT, Duquesnay DL, Topper TH (1988) Notch fatigue behavior of 1045 steel, *Int J Fatigue* 10:109-116.
- [9] Atzori B, Lazzarin P, Meneghetti G (2003) Fracture mechanics and notch sensitivity, *Fatigue Fract Eng Mater Struct* 26:257-267.
- [10] Bazant ZP (1977) Scaling of quasibrittle fracture: asymptotic analysis, *Int J Fract* 83:19-40.
- [11] Tanaka K, Nakai Y, Yamashita M (1981) Fatigue growth threshold of small cracks, *Int J Fract* 17:519-533.
- [12] Livieri P, Tovo R (2004) Fatigue limit evaluation of notches, small cracks and defects: an engineering approach, *Fatigue Fract Eng Mater Struct* 27:1037-1049.
- [13] Tada H, Paris PC, Irwin GR (1985) *The Stress Analysis of Cracks Handbook*, Del Research.
- [14] Meggiolaro MA, Miranda ACO, Castro JTP (2007) Short crack threshold estimates to predict notch sensitivity factors in fatigue, *Int J Fatigue* 29:2022–2031.
- [15] Castro JTP, Meggiolaro MA (2009) *Fatigue v.2*, ISBN 978-1449514709 (in Portuguese)
- [16] Schijve J (2001) *Fatigue of Structures and Materials*, Kluwer.
- [17] Shigley JE, Mischke CR, Budynas RG (2004) *Mechanical Engineering Design*, 7th edn, McGraw-Hill.
- [18] Dowling NE (2007) *Mechanical Behavior of Materials*, 3rd edn, Prentice Hall.
- [19] Miranda ACO, Meggiolaro MA, Castro JTP, Martha LF (2003) Fatigue life prediction of complex 2D components under mixed-mode variable loading, *Int J Fatigue* 25:1157-1167.